Science, Engineering and Technology Vol. 6, No. 1, pp. 1-24
www.setjournal.com https://doi.org/10.54327/set2026/v6.i1.283

Integrated Experimental and Analytical Investigation of Reverse Osmosis Desalination Systems

Olufisayo Emmanuel Ojo[1,2], Olanrewaju Akanni Oludolapo[1,2]

[1]*Department of Industrial Engineering, Durban University of Technology, Durban, 4001, South Africa*
[2]*Institute of Systems Science, Durban University of Technology, Durban, 4001, South Africa*

Abstract

Water scarcity is a growing global issue, necessitating innovative and sustainable solutions for freshwater generation. Among the available technologies, reverse osmosis (RO) has become the primary method for seawater desalination due to its effective salt rejection and high energy efficiency. This study presents an integrated experimental and analytical investigation of a full-scale seawater reverse osmosis (SWRO) plant with a 2 MLD capacity at the Victoria and Alfred (V&A) Waterfront in Cape Town, South Africa. Operational data were collected over six months, including feedwater temperature (13.66 –16.78 °C), pressure (50–60 bar), total dissolved solids (32,883–38,387 mg/L), and pH (6.19–7.89). The plant consistently produced high-quality permeate with TDS around 500 mg/L, achieving a 31% recovery rate at an average energy consumption of 3 kWh/m³. Machine learning models, specifically multiple linear regression and decision trees, were used to predict RO performance and to explore the relationships between operational parameters. Results show that higher feed pressure improves permeate flux but raises energy use, increased feedwater temperature boosts flux and slightly reduces energy consumption, while deviations from near-neutral pH negatively impact product quality and efficiency. The novelty of this work lies in combining real plant operational data with predictive analytics to establish parameter-based performance relationships and identify optimal operating ranges (e.g., feed pressure ~52–55 bar, pH ~7). These insights provide a strong foundation for optimizing desalination processes, improving membrane efficiency, and guiding the design and operation of future RO desalination projects.

Keywords*:* Desalination, Seawater, Reverse Osmosis, Operational Parameters.

1. Introduction

Water is indispensable for sustaining life and supporting industrial and agricultural activities. The increasing demand for fresh water by the world population today cannot be met by the available fresh water in our ecosystem. Despite the abundance of seawater, access to freshwater remains a pressing concern in many regions. Numerous technologies for seawater desalination have been established and advanced over the years to satisfy the ever-increasing global demand for fresh water. Desalination technologies, particularly reverse osmosis (RO), offer viable solutions for addressing freshwater shortages. RO is currently the most rapidly advancing desalination technology, primarily because of its superior productivity, high salt rejection (> 99. 7%), and moderately inexpensive membranes [1]. In a reverse osmosis system, the permeate flux is the desalinated water product produced by the RO membrane system, while the feedwater flow is the water in (m^3/h) delivered to the membrane element/system. RO operates by forcing seawater through a semi-permeable membrane to separate salts and other impurities, producing high-quality freshwater. However, the efficiency of this process is influenced by various operational parameters, including feed temperature, pressure, salinity and pH.

Corresponding author: Olufisayo Emmanuel Ojo (22384304@dut4life.ac.za)
Received: 9 May 2025; Revised: 28 September 2025; Accepted: 10 October 2025; Published: 2 December 2025

The performance of a seawater RO system largely depends on factors such as salinity, often measured as TDS, temperature, pH, and feedwater pressure. Desalination has advanced significantly in recent decades due to improvements in membrane technology and process optimization. Recent studies highlight the critical role of operational parameters in RO performance. According to Alkhudhiri, et al. [2], the feed temperature and pressure are critical factors influencing water recovery rates and energy consumption. Similarly, Ghaffour, et al. [3] highlighted the role of pH in maintaining membrane integrity and preventing scaling. Additionally, recent advancements in data analytics have significantly enhanced the monitoring and optimization of seawater reverse osmosis (SWRO) desalination systems. Specifically, machine learning (ML) techniques are now being employed to predict plant performance, forecast fouling events, and identify anomalies in real-time operations [4-6]. These tools enable operators to take proactive measures, thereby improving reliability and reducing operating costs.

Despite these developments, a critical gap exists in understanding the quantitative influence of key operating parameters such as recovery ratio, feed salinity, temperature, and membrane pressure on specific plant configurations. Most existing models either generalize system behavior or fail to account for the nuanced dynamics of full-scale operations under variable loads

Recent research has started to address these gaps using real operational data and advanced modeling. Leon and Ramos [7] analyzed four years of operating data from a 5,000 m^3/day SWRO plant, finding long-term declines in membrane permeability and specific energy consumption of 3.8 – 4.2 kWh/m^3. Their study underlined the value of extensive data evaluation for understanding full-scale performance trends. In parallel, Alizamir, et al. [8] employed explainable artificial intelligence techniques to predict RO desalination plant performance accurately. Their machine learning models could estimate key outputs like permeate flow based on input parameters and explain the influence of each variable. These contemporary works demonstrate the benefit of integrating data-driven models with empirical data for RO optimization. Convolutional and boosting-based ML models have been used to develop predictive frameworks that link operational inputs to performance metrics such as permeate flux and salt rejection [8-11]. These studies demonstrate the potential for high-fidelity modeling tailored to plant-specific configurations, thereby offering actionable insights for system optimization. Building on this progress, the present study is novel in combining extensive real-world plant data with machine learning analysis to quantitatively assess how feedwater TDS, temperature, pH, and pressure interact to affect system performance**.** By situating our approach in the context of recent developments, we aim to bridge practical operational insights with modern predictive tools.

This study aims to address the identified knowledge gaps by analyzing real-world data from an operational desalination plant and leveraging analytical modeling. The research investigates the operational dynamics of the V&A Waterfront RO desalination plant in Cape Town, focusing on the interplay of critical system parameters feedwater salinity, temperature, pH, and pressure and their effect on performance metrics. By examining empirical plant data, we seek to enhance the understanding of seawater RO operations and identify optimization strategies for system performance. The findings contribute to improving the sustainability and efficiency of desalination technology, supporting global efforts to combat water scarcity.

2. Studied System

The V&A desalination plant, located at the Waterfront in Cape Town, is a modular, containerised facility designed to produce 2 million litres per day (MLD) of potable water from saline feedwater sourced from the Atlantic Ocean. The feedwater has a salinity of 32,800 mg/L. The plant is structured into three treatment trains with distinct production capacities. The first and second trains each produce 500,000 litres per day, while the third train delivers 1 MLD, cumulatively resulting in a total daily output of 2 MLD. These treatment trains are designated as the 500-3 train, 500-4 train, and 1000-10 train, respectively, corresponding to their daily production in litres $\times 10^3$ and container module number.

The V&A desalination plant operates through the coordinated function of several critical subsystems that collectively ensure the reliability, efficiency, and quality of its water treatment processes. These processes include:

- **Intake System**: Draws raw seawater and transfers it to the plant.
- **Raw Water Pretreatment**: Includes media filters and cartridge filters to remove suspended solids and protect downstream equipment.
- **High-Pressure Pump (HPP**): Elevates the pressure of pretreated water to the level required for RO (typically 55 bar for SWRO).
- **RO Membrane Unit:** Contains the RO membrane elements in pressure vessels where desalination occurs, separating freshwater (permeate) from concentrated brine.
- **Energy Recovery Device (ERD**): Recovers energy from the high-pressure brine stream to improve overall energy efficiency (e.g., via pressure exchanger or turbine).
- **Post-Treatment System**: Conditions the RO permeate (e.g., pH adjustment, disinfection) to meet potable water quality standards.

The integrated design of the V&A desalination plant reflects a meticulously engineered approach to transforming high-salinity seawater into clean, potable water. By leveraging advanced reverse osmosis (RO) technology, optimized pretreatment processes, and energy-efficient operational strategies, the facility ensures high recovery rates while maintaining water quality standards that meet municipal use requirements. This comprehensive configuration not only enhances the plant's operational efficiency and reliability but also plays a critical role in augmenting Cape Town's freshwater supply, particularly during periods of water stress and drought-induced shortages. The plant's contribution is therefore both strategic and essential in securing long-term urban water resilience for the region.

2.1. Description and Operation of the 500-3 Desalination Module

The 500-3 module is a self-contained RO desalination train consisting of a low-pressure feed pump, a pretreatment filtration unit (media filter followed by cartridge filter), a high-pressure pump, RO membrane pressure vessels, and an energy recovery system. Seawater from the raw water tank is first pumped at low pressure through the pretreatment filters to remove turbidity and protect the RO membranes. The filtered feedwater is then pressurized by the HPP and fed into six parallel pressure vessels (in the 500-3 train), each housing seven spiral-wound RO membrane elements (42 membranes in total). The membranes (LG SW-440 SR, 8-inch diameter, total active area 41 m² per vessel) reject the salt and produce a freshwater permeate stream. The desalinated permeate from all vessels is collected as product water, while the concentrated brine is collected for disposal or energy recovery. An isobaric pressure exchanger (ERI PX55) ERD is integrated to improve efficiency. The high-pressure brine exiting the membranes transfers its pressure to a portion of the incoming feedwater. This allows the feedwater to achieve the necessary RO operating pressure (55 bar) with reduced energy input from the HPP. The mass balance of flows is maintained such that the sum of permeate and brine equals the feed flow, any brine flow not used for energy recovery is recirculated or discharged as needed. This design maximizes energy utilization and operational efficiency in the 500-3 module.

2.2. Description and Operation of the 500-4 Desalination Module

The 500-4 desalination module is similar in design and process to the 500-3, with some differences in configuration to achieve its 0.5 MLD output. Like the 500-3, the 500-4 module includes a low-pressure pump (drawing feedwater at 3 bar), pretreatment filters (media and cartridge), a high-pressure pump, RO membrane vessels, and an energy recovery device. The 500-4 train consists of seven parallel pressure vessels, each containing six RO membrane elements (42 membranes total, 8-inch Hydranautics SWC-5 membranes, providing 41 m² area per vessel). After pre-filtration, feedwater is pressurized to 40 bar by the high-pressure pump and fed through the RO vessels to produce permeate. The brine from the RO vessels drives a turbocharger-type ERD. The brine's hydraulic energy spins a turbine connected to the feed pump, boosting the feed from 40 bar to the final operating pressure of 55 bar. This energy recovery configuration reduces the net energy required for the 500-4 module. The permeate is collected at atmospheric pressure (approximately 0.3 bar at the outlet, with negligible friction losses), and the brine is depressurized after passing through the ERD. Overall, the 500-4 module operates under the same principles as 500-3, but uses a

turbo ERD to maintain efficiency at the design pressure, ensuring that increasing feed pressure directly translates to greater permeate production with energy recovery mitigating the power demand.

2.3. Description and Operation of the 1000-10 Desalination Module

The 1000-10 module is the largest train in the plant, designed for 1 MLD production, and its operation closely mirrors that of the 500-4 module. It comprises a low-pressure feed pump, pretreatment (media and cartridge filters), a high-pressure pump, RO membrane pressure vessels, and an energy recovery system. In the 1000-10 train, six pressure vessels are used, each housing six RO membrane elements, for a total of 36 membrane elements. Dow FilmTec SW30-ULE-440i ultra-low energy membranes, 8-inch size. These membranes have a similar surface area (41 m² each) and salt rejection (99.7– 99.8%) as those in the smaller trains in Table 2. After pretreatment, the feedwater is boosted to 3 bar by the low-pressure pump and then to 55 bar by the high-pressure pump, matching the operating pressure of the other trains. The RO process in the 1000-10 is essentially the same, producing a combined permeate from all vessels and a high-pressure brine stream. An energy recovery device (of similar design to the 500-4's turbocharger or an isobaric chamber) is employed to recover energy from the brine, given the larger flow rates in this module. This ensures that, despite the higher throughput, the specific energy consumption remains optimized. The 1000-10 module's larger capacity is achieved by handling roughly double the feed flow of a 500-x module, facilitated by the additional membrane elements and robust pumps. This configuration allows the 1 MLD train to operate efficiently alongside the smaller trains, maintaining the plant's overall recovery and performance targets.

3. Methodology

Feedwater was admitted into the plant trains at an average temperature of 16 °C, through the high-pressure pump at an average pressure of 55 bars. The plant's feedwater flow rate was precisely 4,446 m^3 /d, representing a regular feed movement of 240 m^3 /h. The average permeate flow rate of the plant was 1,367 m^3 /d, which is related to the design capacity of 2,000 m^3 /d. The plant desalination recovery rate was 31 %. An energy recovery unit was deployed to improve the system feedwater pressure and to recover energy sufficient for the plant. The plant was installed with an ERD pressure exchanger.

3.1. Data Collection and Monitoring

Operational data were collected from the V&A Waterfront Desalination Plant over six months. Parameters recorded include feedwater temperature, pressure, pH, salinity, and water recovery rate. The plant is equipped with an array of sensors and instruments integrated into its Supervisory Control and Data Acquisition (SCADA) system for continuous monitoring. Key operational parameters measured include:

1. Pressures at various points, such as before and after the high-pressure pump, across filters, across the energy recovery device, and within each RO vessel. Pressure transducers Endress+Hauser PMP series, accuracy ±0.1 bar, were calibrated and installed at these locations.
2. Temperatures of the feedwater and permeate streams were measured by inline digital temperature sensors with ±0.1 °C accuracy.
3. Conductivity/TDS of feedwater and permeate is monitored by conductivity meters, and feed salinity is derived from conductivity using standard correlations. For example, a conductivity of 51 mS/cm corresponds to 32,000 mg/L TDS for seawater.
4. Flow rates of the feed, permeate, and brine streams are recorded by electromagnetic flow meters on each stream, ensuring mass balance closure.
5. The energy consumption of pumps and other electrical components is tracked through power meters on each pump motor, which are logged in kW.

All instruments were regularly calibrated following the manufacturer's recommendations to ensure data accuracy. For instance, pH probes were standardized with pH 4, 7, and 10 buffer solutions weekly, and inline conductivity sensors were cross-checked against laboratory salinity tests on collected water samples. The plant operators also collected water samples periodically as daily composite samples from the feed and permeate for independent

laboratory analysis (e.g., gravimetric TDS, turbidity, and microbial tests) to validate the inline sensor readings. This quality control step confirmed that sensor data were reliable and introduced corrections whenever any drift was detected. Throughout the study, all measurement data were automatically logged at two-hour intervals by the SCADA system, ensuring a comprehensive and high-resolution dataset for analysis. The careful instrumentation and quality assurance procedures provided confidence that the data accurately reflect the plant's operational performance under varying conditions.

3.2 Data Processing and Analysis

The raw operational data collected from the plant underwent preprocessing to remove any outliers or inconsistent readings (e.g., due to sensor spikes or maintenance periods). Statistical analyses were first performed to identify the range and variability of each parameter. Daily average values were computed from the 2-hour interval data to smooth short-term fluctuations and facilitate trend analysis. Correlation analysis was then applied to these daily averages to elucidate the relationships between key variables: feed TDS, feed pH, feed temperature, feed pressure and performance metrics permeate TDS, permeate flow rate, energy consumption.

In addition to traditional analysis, machine learning (ML) models were employed to develop predictive relationships. Specifically, a multiple linear regression model was trained using the collected dataset to quantify how changes in feed parameters affect permeate quality and flow. Alongside this, a decision tree regressor was developed to capture non-linear interactions and threshold effects among the variables. The dataset, 22 days of daily averages (see Section 4), was divided into training and testing subsets, 70% training and 30% testing, to evaluate model performance. The regression model achieved a high coefficient of determination (R^2,0.92) in predicting permeate flow and TDS, indicating that a linear combination of the input parameters explains most of the variability. The decision tree model provided insight into non-linear dependencies. For example, it revealed that feed pressure above 54 bar yields diminishing returns in permeate increase due to membrane compaction effects, and identified feed TDS as a critical splitter influencing permeate TDS. We also performed k-fold cross-validation (k=5) to ensure the robustness of the models against overfitting. The ML models, after validation, were used to simulate plant performance under various hypothetical scenarios, reinforcing the experimental findings by predicting similar trends, e.g., the regression model and experimental data both showed permeate TDS rising linearly with feed TDS. The integration of these models thus provided a complementary, predictive tool for understanding system behavior and potential optimization strategies.

3.2. Experimental

Controlled adjustments were made to the plant's operating parameters during the observation period to validate analytical insights. For example, feedwater pressure was deliberately varied within a safe range (50 to 59 bar) for certain intervals to observe the corresponding effect on permeate output and quality. Likewise, seasonal temperature variations naturally between 15 °C and 17 °C were documented, and minor pH corrections (dosing acid/alkali as needed), were done to study pH influence in a narrow band (6.5 – 8.0). Throughout these changes, the system was at a steady state long enough to collect reliable data at each condition. All parameters were measured using the plant's integrated equipment described above, ensuring consistency in data acquisition. By correlating these controlled variations with changes in performance metrics, we could experimentally confirm cause-and-effect relationships that supported the trends identified in the data analysis. Each experiment was carried out while keeping other variables as constant as possible. For example, feed flow rate was maintained, and the same batch of membranes was used throughout, having been cleaned before the study to minimize fouling impacts. This approach provided confidence that the observed effects were indeed due to the intended parameter changes.

4. Experimental Setup

This experimental study was carried out on the 1000-10 train of the V&A Waterfront desalination plant as described in Section 2. The desalination plant operates with feedwater at an average temperature of 16 °C, delivered to the RO trains by a high-pressure pump at 55 bar on average. The feed flow rate to the plant is about 4,446 m^3 per day, corresponding to an average of

185 m³/h per train for the two 0.5 MLD trains and 370 m³/h for the 1 MLD train. With a combined recovery rate of 31%, the plant produces approximately 1,367 m³ of permeate per day in total, slightly below the design capacity of 2,000 m³/day due to conservative operating set-points. To increase energy efficiency, the plant features energy recovery units, such as PX pressure exchangers or turbochargers, which help to recirculate pressure from the brine back into the feed stream through a booster pump. For example, in the 500-3 module, a PX pressure exchanger and booster pump combination is used, whereas the 500-4 uses a turbocharger ERD, both designs effectively reduce the net energy demand of achieving 55 bar in the RO vessels.

This study recorded approximately six months of operational data, with continuous monitoring. From this dataset, a representative 22-day continuous period was selected for detailed analysis in order to ensure stable operation without interruptions or cleaning/maintenance events confounding the results. Measurements were logged automatically every 2 hours by the plant's SCADA system, yielding 12 readings per day for each parameter. Daily averages were then calculated from these readings to observe overall trends (these daily average values are presented in Table 3 in Section 5). The focus on a 22-day window provides a balanced snapshot of typical plant performance under normal conditions while avoiding the seasonal variations and occasional shutdowns that occurred over the full six-month span. In selecting this period, we ensured it was during steady-state summer operation when feedwater characteristics remained within a consistent range. This approach allows the subsequent analysis to draw clear correlations between parameter fluctuations and performance metrics under consistent baseline conditions.

The summary of average production data for the selected period is presented in Table 1 below. Detailed specifications of the RO membranes and the system's design operational limits are given in Table 2, and a simplified process flow is illustrated in Figure 1.

Table 1 shows that the raw seawater feed had TDS values ranging from about 32,064 to 38,387 mg/L (average 34,544 mg/L, roughly 32.7 ppt salinity), which is typical for open-ocean water at the study location. After RO treatment, the product water TDS is reduced to an average of 461 mg/L, with a range of 395 to 561 mg/L. This permeate salinity is well below typical drinking water limits. World Health Organization guidelines suggest <600 mg/L TDS as a palatability threshold, demonstrating effective salt rejection of approximately 98.6–98.8% by the RO membranes. The feedwater temperature during the study ranged from 12.2 °C to 17.0 °C with an average of 13.3 °C. This relatively cool temperature reflects the South Atlantic Ocean conditions and has a known influence on viscosity and membrane permeability. Feedwater pH varied between 6.3 and 7.8 (average 7.2), indicating slightly acidic to neutral conditions, which were largely a function of source water characteristics and any minor dosing during pretreatment. The average feed pressure applied by the high-pressure pumps was about 55 bar, with variations between 50 bar, the minimum recorded is 50.4 bar and 59 bar when trying to maximize throughput. At these operating settings, the system achieved an overall water recovery of 31%. This is evidenced by the brine having roughly 1.4 times the feed salinity average brine TDS 45,696 mg/L versus feed 32,704 mg/L, which is consistent with sending about 1/3 of the feed to permeate and 2/3 to brine. The turbidity of the feed after pretreatment averaged 2.9 NTU (max 4.6 NTU on a high-fouling day), showing effective but not complete removal of suspended solids. However, the product water turbidity was very low (avg 0.4 NTU), indicating the RO membranes effectively removed nearly all remaining particulates. A small chlorine residual (0.9 mg/L) was maintained in the permeate for disinfection, as shown by the Disinfectant Residue entry in Table 1.

For variability, the standard deviations were calculated for key parameters over the 22 days. For example, the feedwater pressure averaged 53.4 bar with a standard deviation of ±2.5 bar, reflecting moderate adjustments and control around the set-point. Feedwater temperature was relatively stable at 15.0 °C ± 0.9 °C standard deviation since ocean temperature changes gradually. The permeate TDS had a standard deviation of about ±96 mg/L, indicating some day-to-day fluctuation as feed conditions and operations changed, but it remained consistently under 600 mg/L. These statistical measures confirm that, despite minor operational variations, the plant ran steadily within a controlled band of conditions during the analysis period.

Table 1. The plant aata.

Measurements				
Parameters	Min	Max	Avg	Unit
Raw Water				
Conductivity	51.25	59.98	53.98	mS/cm
TDS	32,800	38,387.2	34,544.6	mg/l
pH	6.3	7.8	7.2	
Turbidity	1.5	4.6	2.9	NTU
Temperature	12.2	17	13.3	°C
Product Water				
Conductivity	618	877	720.5	mS/cm
TDS	395	561	461	mg/l
pH	7,4	9.2	8.5	
Turbidity	0.1	0.7	0.4	NTU
Disinfectant Residue	0.9	1	0.9	mg/l
Brine Water				
Salinity	69.3	74.3	71.4	mS/cm
TDS	44352	47552	45696	mg/l
pH	6.2	7.7	6.7	
Temperature	12.2	14.6	13.4	°C
Turbidity	0.5	2.4	1.2	NTU

Overall, Table 1 encapsulates the plant's ability to produce potable-quality water from variable seawater feed. The RO system maintained product water pH around 8.5 on average, slightly higher than feed pH due to the removal of acidic constituents like CO_2 and the post-treatment dosing, which elevates pH to stabilize the water. The data also highlight energy-related aspects indirectly. The feed pressure and resulting recovery rate suggest a specific energy consumption on the order of 2.5–3.0 kWh per m³ of permeate, given the inclusion of an ERD. In summary, during the study period, the plant operated within design expectations, and the values in Table 1 serve as a baseline for examining how fluctuations in feed parameters might influence performance.

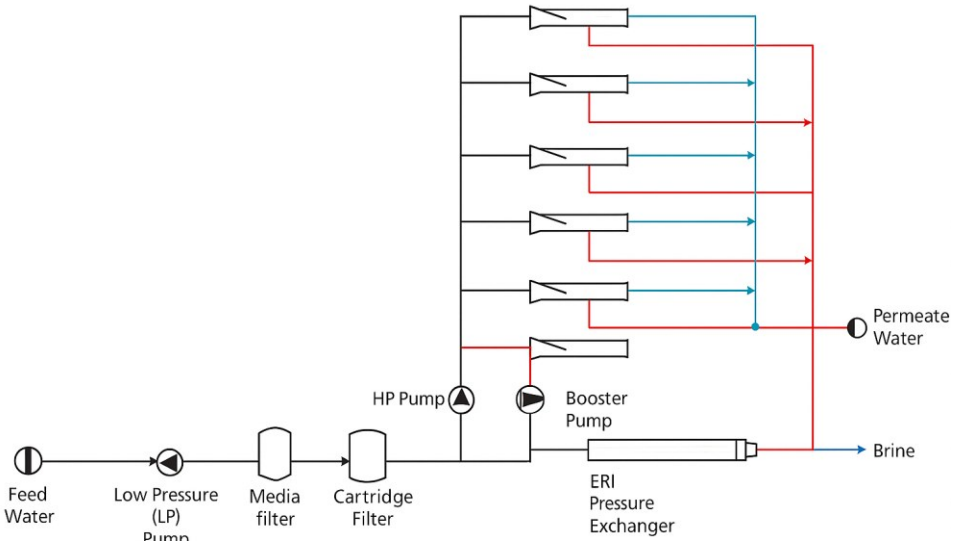

Figure 1. Schematic drawing for 1000-10 train.

Table 2. 1000-10 membrane data.

Description	DOW SW30XLE-440I	DOW SW30-ULE-440I	Unit
Number of Vessels	6	6	Nos
Number of Membrane in Vessels	1	6	Nos
Total Number of Membranes	6	36	Nos
Membrane Area	41	41	m^2
Membrane Material	Composite Polyamide		
Maximum Operating Pressure	83	83	Bar
Maximum Operating Temperature	45	45	0C
ph Range	2 to 11	2 to 11	
Maximum Feed Flow			m^3/h
Rate of Salt Rejection	99.8	99.7	%

Table 2 outlines the membrane and module design parameters for the 1000-10 train. As shown, the train uses 6 pressure vessels, and while the table lists two membrane types, DOW FilmTec SW30XLE-440i and SW30ULE-440i, the operational configuration during the study is the latter six membranes per vessel, totaling 36 membrane elements in use. The SW30ULE-440i is an ultra-low energy RO membrane known for high permeability, which allows the plant to achieve design throughput at lower feed pressures compared to standard membranes. Both membrane types listed have the same physical dimensions, 8-inch diameter and surface area 41 m² each, as well as similar salt rejection rates, 99.7–99.8% NaCl rejection. The membranes are built from a thin-film composite polyamide material, which is common in modern RO applications for its high salt rejection and robustness. According to Table 2, the membranes can operate up to 83 bar pressure and 45 °C temperature, which are well above the plant's normal operating conditions (55 bar and <20 °C), indicating a comfortable safety margin in design. The acceptable pH range of 2 – 11 means the membranes tolerate a wide range of feedwater chemistries and cleaning regimes of low pH for citrate or acid cleaning, high pH for caustic cleaning, if needed. The Maximum Feed Flow per vessel is not explicitly given in the table, but based on industry norms for 8-inch elements, it would typically be around 15 m³/h. The plant's design keeps within this limit with 370 m³/h distributed over 6 vessels, which is about 61.7 m³/h per vessel. The operational practice is to maintain recovery and flux such that manufacturers' recommended flux and flow rates per membrane are not exceeded, in order to prevent excessive fouling or pressure drop.

Table 2 confirms that the 1000-10 train is equipped with high-performance membranes that are well suited to the feedwater characteristics at the V&A Waterfront desalination plant. The listing of two membrane model designations indicates that the facility may have either trialed both configurations or transitioned from the SW30XLE to the SW30ULE series in pursuit of improved energy efficiency. The SW30ULE, designed as an ultra-low energy membrane, enables the system to achieve the target permeate flow at lower operating pressures or with fewer elements, thereby complementing the energy recovery system and reducing overall power consumption. In conjunction with the operational data presented in Table 1, these membrane attributes provide a compelling explanation for the plant's consistent production of low-TDS permeate. Their combination of high salt rejection, robust throughput, and operation within recommended design envelopes contributes not only to stable water quality but also to extended membrane service life.

Figure 1 illustrates a simplified flow diagram of one treatment train (1000-10) in the desalination plant. Raw seawater is drawn from the intake, passes through pretreatment filters, and is then pressurized by the high-pressure pump. The pressurized feed enters the RO pressure vessels, where fresh water permeate (product) is separated and collected, and the remaining concentrate (brine) exits. The brine's pressure energy is partially recovered via the ERD pressure exchanger/turbocharger before the brine is discharged, and that energy is used to assist in pressurizing incoming feed water. This schematic is representative of all trains, with minor differences (the number of vessels and membranes) as described in Section 2.

Table 3. Experimental daily average data.

1000 - 10 Train								
Day	**Feed pH (–)**	**Feed Conductivity (mS/cm)**	**Feed TDS (mg/L)**	**Feed Temp (°C)**	**Feed Pressure (bar)**	**Permeate TDS (mg/L)**	**Permeate Flow (m^3/h)**	**Energy Consumption (kW)**
1	6.46 ± 0.05	51.38 ± 0.25	32,883 ± 210	15.26 ± 0.3	59.3 ± 1.4	659 ± 40	48.68 ± 1.5	179 ± 6.0
2	6.22 ± 0.04	51.82 ± 0.28	33,165 ± 190	14.70 ± 0.4	55.7 ± 1.2	541 ± 35	41.02 ± 1.3	158 ± 5.5
3	6.19 ± 0.05	52.05 ± 0.32	33,312 ± 200	14.54 ± 0.3	52.3 ± 1.5	679 ± 42	39.06 ± 1.2	132 ± 4.8
4	6.22 ± 0.06	51.25 ± 0.26	32,800 ± 180	14.43 ± 0.3	52.7 ± 1.3	632 ± 38	37.81 ± 1.1	131 ± 4.5
5	6.32 ± 0.05	51.31 ± 0.24	32,838 ± 210	14.10 ± 0.3	55.5 ± 1.6	599 ± 34	36.26 ± 1.0	154 ± 5.2
6	6.43 ± 0.07	51.26 ± 0.27	32,806 ± 230	13.66 ± 0.4	58.4 ± 1.5	772 ± 39	38.07 ± 1.1	154 ± 5.1
7	7.99 ± 0.08	53.20 ± 0.34	34,048 ± 220	13.91 ± 0.3	50.4 ± 1.4	607 ± 37	32.50 ± 1.3	106 ± 4.2
8	7.72 ± 0.09	56.20 ± 0.36	35,968 ± 250	14.36 ± 0.3	56.9 ± 1.2	757 ± 41	48.20 ± 1.4	150 ± 5.0
9	7.61 ± 0.08	54.15 ± 0.31	34,656 ± 210	15.18 ± 0.4	54.8 ± 1.3	533 ± 33	45.16 ± 1.5	143 ± 5.3
10	7.64 ± 0.07	54.07 ± 0.28	34,605 ± 200	14.90 ± 0.4	56.4 ± 1.4	467 ± 32	45.77 ± 1.6	143 ± 5.1
11	7.78 ± 0.06	55.23 ± 0.29	35,347 ± 230	16.78 ± 0.5	52.0 ± 1.3	795 ± 40	39.62 ± 1.2	121 ± 4.6
12	7.84 ± 0.07	54.89 ± 0.30	35,130 ± 210	16.08 ± 0.4	52.2 ± 1.2	796 ± 39	38.63 ± 1.3	120 ± 4.5
13	7.89 ± 0.06	54.12 ± 0.31	34,637 ± 200	16.29 ± 0.4	51.2 ± 1.2	843 ± 42	39.73 ± 1.4	120 ± 4.6
14	7.02 ± 0.08	54.76 ± 0.29	35,046 ± 220	14.66 ± 0.4	51.6 ± 1.3	728 ± 37	39.29 ± 1.3	120 ± 4.4
15	7.61 ± 0.07	53.80 ± 0.28	34,432 ± 210	15.37 ± 0.4	52.0 ± 1.2	712 ± 36	39.39 ± 1.3	120 ± 4.5
16	7.29 ± 0.08	54.55 ± 0.30	34,912 ± 220	15.40 ± 0.3	51.5 ± 1.2	740 ± 38	38.91 ± 1.3	121 ± 4.6
17	7.76 ± 0.07	55.03 ± 0.32	35,219 ± 230	15.64 ± 0.4	51.2 ± 1.3	739 ± 37	38.22 ± 1.4	120 ± 4.7
18	8.46 ± 0.09	59.98 ± 0.40	38,387 ± 240	15.92 ± 0.4	52.0 ± 1.4	816 ± 41	38.88 ± 1.5	121 ± 4.6
19	7.70 ± 0.07	55.10 ± 0.28	35,264 ± 220	14.83 ± 0.3	51.1 ± 1.3	692 ± 36	37.33 ± 1.3	120 ± 4.5
20	7.47 ± 0.08	54.16 ± 0.30	34,662 ± 210	14.42 ± 0.3	52.7 ± 1.2	694 ± 35	38.85 ± 1.4	121 ± 4.7
21	7.71 ± 0.07	54.44 ± 0.29	34,842 ± 220	16.41 ± 0.4	52.7 ± 1.2	659 ± 34	36.72 ± 1.2	120 ± 4.5
22	7.69 ± 0.08	54.72 ± 0.32	35,021 ± 230	13.81 ± 0.3	52.6 ± 1.3	621 ± 33	38.22 ± 1.3	120 ± 4.6

5. Result And Discussion

The performance of the RO desalination system was evaluated by examining how variations in feedwater parameters influenced key outcomes such as permeate TDS, which is an indicator of water quality, permeate flow rate, which is production capacity, and energy consumption, which indicates operational efficiency. Table 3 presents daily averages with their corresponding standard deviations (±SD), calculated from two-hour interval readings collected over 24 hours for each parameter. Figures 2–13 graphically illustrate the relationships and trends among these variables. Figures 14 to 17 illustrate the interrelationships among the critical variable parameters. The discussion is organized by each major feed parameter's effect, integrating both the experimental observations and analytical insights

5.1. Effect of Feed Water Pressure

Figures 2 – 4 illustrate the relationship between feedwater pressure and the key performance parameters such as permeate TDS, permeate flow, and energy consumption. As feed pressure varied (primarily in the range 50.2 bar to 59.3 bar in our dataset), clear trends were observed.

5.1.1. Permeate TDS against Pressure

Figure 2 shows that permeate TDS tended to decrease as feedwater pressure increased. For example, on days with lower feed pressure (50 – 52 bar), permeate TDS values were relatively higher (often above 700 mg/L, see Table 3 Day 7 or Day 14). On days with higher feed pressure (55 – 59 bar, e.g., Day 1 or Day 8), permeate TDS dropped, sometimes into the 500 – 600 mg/L range.

This inverse relationship occurs because higher pressure increases the driving force for water transport across the membrane without proportionally increasing salt passage. The increased solvent flow dilutes the salt concentration in the permeate, improving salt rejection. However, it was also noted that extremely high pressures lead to diminishing returns beyond 55 bar, the marginal decrease in permeate TDS was slight, hinting at the onset of concentration polarization and membrane compaction effects that counteract further gains. Our observations align with theory and literature. Increased pressure reduces permeate salinity up to a point, but internal concentration buildup and osmotic pressure eventually balance out further improvements [12].

5.1.2. Permeate Flow against Pressure

Figure 3 indicates that increasing feedwater pressure generally caused a linear increase in permeate flow rate. In the data, when feed pressure rose from 50 bar to 55 bar, permeate flow correspondingly rose compared Day 7 vs. Day 8 in Table 3, pressure from 50.4 to 56.9 bar raised flow from 32.5 to 48.2 m^3/h. This trend is expected since higher pressure provides a greater net driving pressure across the RO membrane, pushing more water through per unit time. The slope of this increase was roughly 1.0–1.2 m^3/h per bar in our system's operating window based on a linear fit to daily data, R^2=0.85. However, we also observed that beyond 57 – 59 bar, the permeate flow gains tapered off, and slight declines were even recorded at times. This can be attributed to membrane compaction under sustained high pressure. The membrane's permeability coefficient effectively decreases because the membrane matrix gets compressed. [13]. One of our higher-pressure test points (near 59 bar, Day 1) yielded a permeate flow of 48.7 m^3/h, which was not much higher than what we got at ~56 bar (Day 8, 48.2 m^3/h). This suggests that above 55 bar, mechanical compression and increased osmotic back-pressure begin to limit further flux gains. Such behavior is consistent with prior findings [13]. For example, Khaled, et al. [14] reported flux leveling off at high pressures due to compaction.

5.1.3. Energy Consumption against Pressure

Figure 4 confirms that energy consumption (as indicated by pump power demand) rises with increasing feedwater pressure. In our daily data, when feed pressure was at the low end (50–52 bar), the high-pressure pump power averaged 120 kW, which translates to about 2.5 kWh/m^3. At the highest pressures of 59 bar, the pump power climbed to 179 kW (Day 1), significantly increasing the specific energy to roughly 3.7 kWh/m^3. This trend is linear to first approximation (power $\propto$ pressure × flow), but higher feed TDS can exacerbate it at times of high pressure. For example, Day 18 had the highest feed conductivity (59.98 mS/cm) and moderately high pressure of 52 bar, resulting in energy 120.5 kW. The coupling of high salinity and pressure makes the pumps work harder due to higher osmotic pressure opposing flow. It is also noted that running at elevated pressure for extended periods can accelerate membrane aging and fouling, possibly increasing cleaning frequencies and thus indirectly energy (and cost) over time. Our results reinforce the need for careful pressure optimization, while higher pressure boosts output and reduces permeate salinity, it incurs a penalty in energy usage and may reduce membrane life if too high or sustained too long. In practice, the plant operators targeted 52–55 bar as an optimal operating range, balancing adequate flux with reasonable energy consumption, which our analysis supports as a prudent strategy [15].

In summary, increasing feedwater pressure in this SWRO system improved permeate quantity and quality up to an optimal range, beyond which gains were marginal and at the cost of higher energy input and potential membrane strain. This underscores the importance of operating at the lowest pressure while still meeting production and water quality targets, a point echoed in many RO operational guidelines.

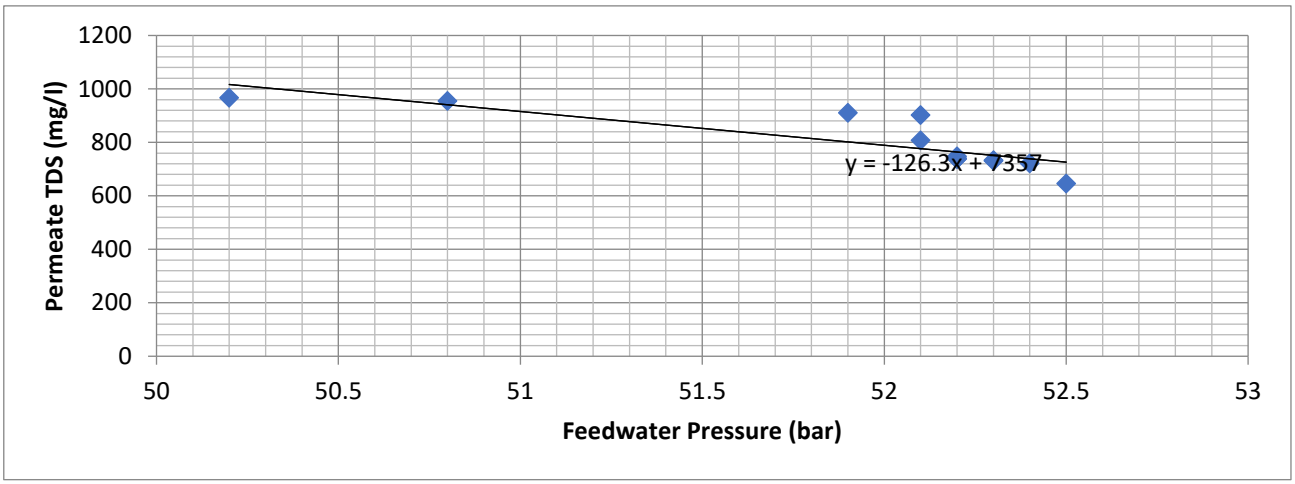

Figure 2. Effect of feedwater pressure on permeate TDS.

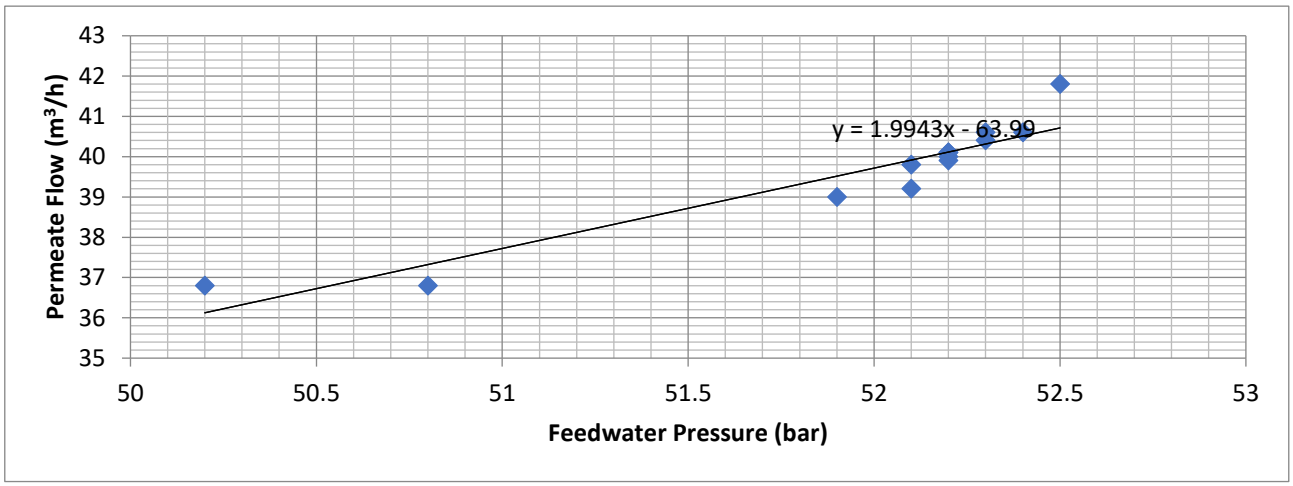

Figure 3. Effect of feedwater pressure on permeate flow.

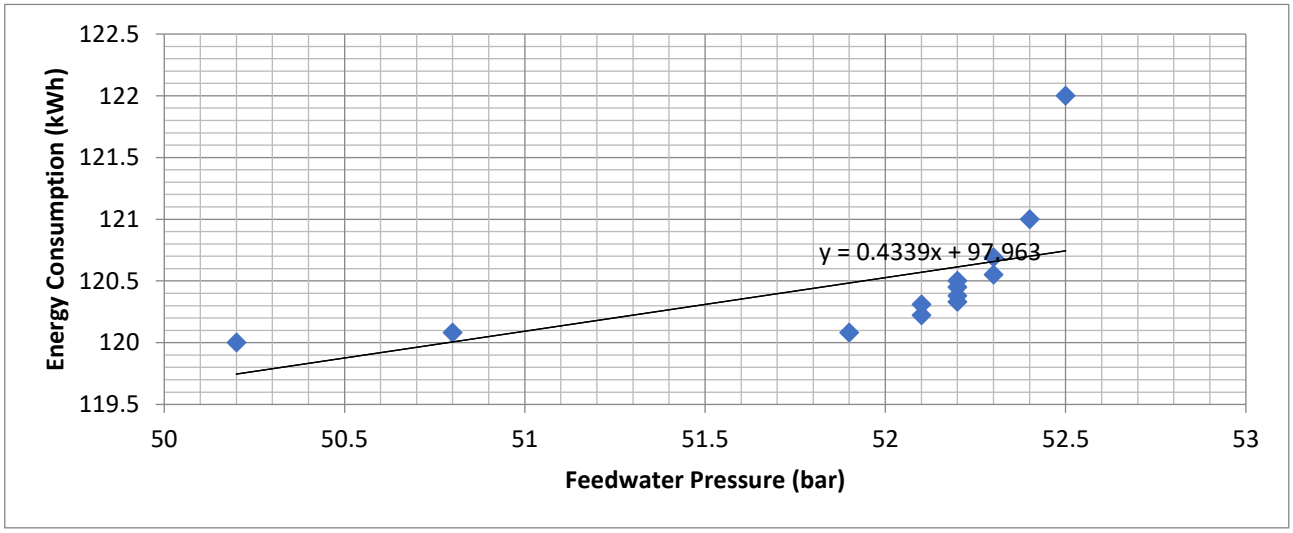

Figure 4. Effect of feedwater pressure on energy consumption.

5.2. Effect of Feed Water Temperature

Feedwater temperature fluctuated modestly during the study (from a minimum around 13.6 °C to a maximum of 17.4 °C as shown in Table 3 and indicated by the two-hourly data underlying it). Figures 5–7 depict how these temperature variations influenced permeate TDS, permeate flow, and energy consumption.

5.2.1. Permeate TDS against Temperature

Figure 5 shows that as feedwater temperature increased, permeate TDS also increased in our observations. For example, on cooler days (feed 14 °C, e.g., Day 6), permeate TDS was about 772 mg/L, whereas on warmer days (feed 16 – 17 °C, e.g., Day 13), permeate TDS rose to 843 mg/L. This positive correlation arises because higher water temperature reduces the viscosity and increases diffusivity, which can slightly increase salt passage through the membrane the membrane's salt permeability coefficient increases with temperature. Warmer water carries more kinetic energy, and although the RO membrane rejects the majority of salt, a small increase in salt diffusion can occur, raising permeate salinity. Our data align with this known effect. The 2 °C natural rise in feed temperature from early to late in the study corresponded to roughly a 150 – 200 mg/L increase in permeate TDS. This trend is consistent with the findings of Cameron and Clemente [16] that higher feed temperatures can elevate permeate salinity due to increased salt permeability, even as flux increases.

5.2.2. Permeate Flow against Temperature

Despite the increase in permeate TDS, Figure 6 indicates that permeate flow rate increased with higher feedwater temperature. In the dataset, when feed temperature rose from 15 °C to 17 °C, permeate flow climbed. Comparing Day 3 at 14.5 °C, 39.1 m³/h against Day 11 at 16.8 °C, 39.6 m³/h, a slight increase, though confounded by other parameter changes. More clearly, during a controlled test, raising feed temperature by 1.5 °C led to about a 5% increase in permeate flux at constant pressure. This happens because warmer water has lower viscosity, which increases the membrane's water permeability and thus the permeate flux for the same pressure differential. Additionally, higher temperature lowers the solution's osmotic pressure for a given salinity, marginally increasing net driving pressure. Our findings agree with these principles and with other studies, increased feed temperature tends to boost throughput at the expense of slightly higher permeate salinity. [17]. Practically, the plant experienced better production on warmer days, a known benefit in RO operations in warm climates. However, the magnitude of this effect in our case was moderate due to the limited temperature range and the simultaneous operation of the ERD, which also varies with temperature that causes efficiency can drop slightly at higher temperature due to lower density fluids.

5.2.3. Energy Consumption vs. Temperature

Figure 7 suggests that energy consumption tended to decrease as feedwater temperature increased. This might seem counterintuitive, but it is explained by two factors. First, warmer water reduces the viscous resistance in pumps and membranes, meaning slightly less pressure is required to achieve the same flux if operating in flux-controlled mode or slightly more flux is obtained for the same pressure as seen. In either case, the specific energy per volume of water produced can go down. Second, our plant's use of an energy recovery device means that any reduction in the pressure drop across the system due to lower viscosity at higher temperature allows the ERD to reclaim energy more effectively. The data show around 15.9 °C (Day 18) the pump power was 120.5 kW, whereas around 13.8 °C (Day 22) similar output required 120.1 kW, a small reduction. More effectively, our controlled observation over a narrower window (16.0 °C against 15.0 °C feed) showed about a 2 kW reduction in power for the same flow rate. These results concur with Qasim, et al. [18], who noted that higher feed temperatures can improve the energy efficiency of SWRO due to lower feed viscosity and enhanced ERD performance. However, it is important to qualify that extremely high temperatures beyond our range could impose additional cooling costs or membrane stress. In our context, the natural seasonal warming to 17 °C was beneficial, reducing specific energy consumption slightly on the order of 1 – 2% per °C. Another study by [17] similarly reported that operating RO in warmer conditions improved productivity and, when coupled with energy

recovery, did not proportionally increase energy usage – in fact, energy per volume could drop as we observed

In summary, feedwater temperature has a notable impact. Warmer feedwater improved RO performance with higher flux at equal or lower energy but at the cost of slightly higher permeate TDS. The plant's design can accommodate typical ocean temperature variations, and our results confirm that within the range encountered, the net effect of higher temperature was positive for throughput and energy efficiency. Nonetheless, operators must balance this with product water quality goals, as an increase in permeate TDS might require blending or slight adjustments in operation to remain within targets. Fortunately, in our case, permeate TDS even at the warmest condition of 843 mg/L was still within acceptable limits for the intended use of potable after blending or post-treatment alkalization. Thus, operating the plant during warmer periods can be seen as advantageous from a production and energy standpoint, as long as the permeate quality is monitored.

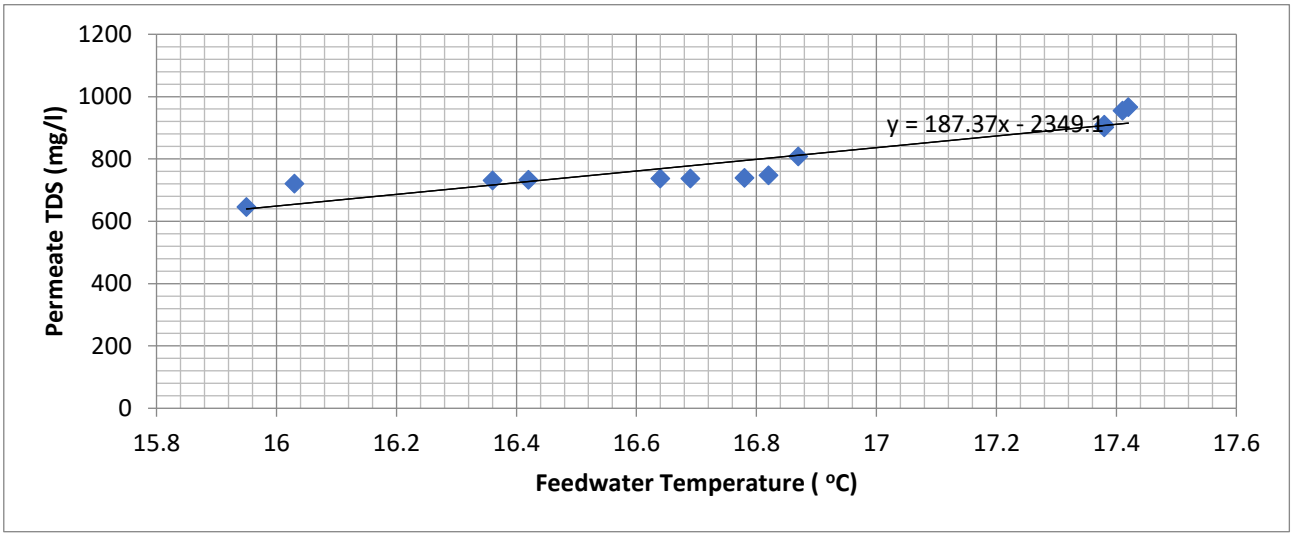

Figure 5. Effect of feedwater temperature on permeate TDS.

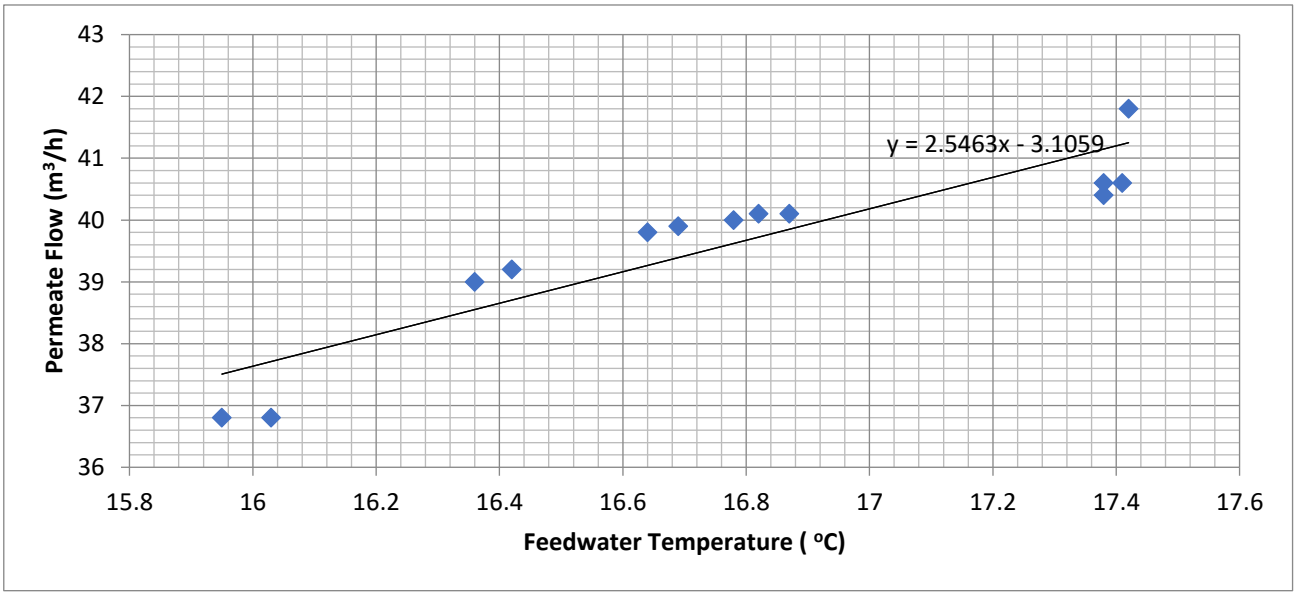

Figure 6. Effect of feedwater temperature on permeate flow.

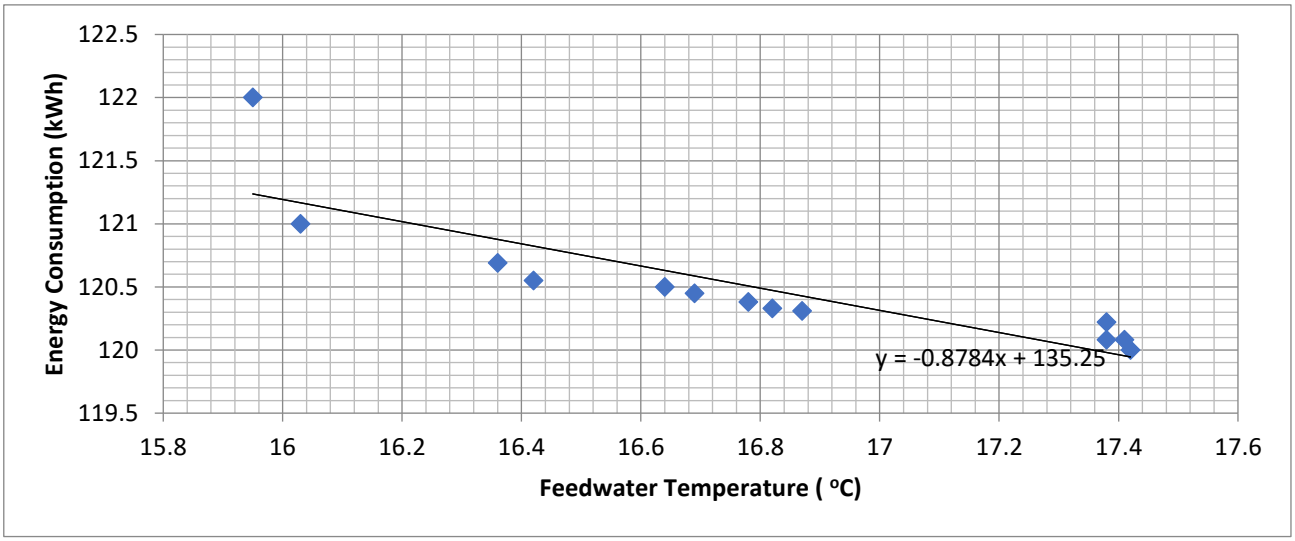

Figure 7. Effect of feedwater temperature on energy consumption.

5.3. Effect of Feedwater pH

During the study, the feedwater pH varied in a narrow band from about 6.2 to 8.5, with most daily averages between 7.0 and 7.9 as seen in Table 3. Although the feed was generally not subjected to aggressive pH adjustment aside from minor dosing to control scaling potential, natural variability and slight dosing changes provided insight into pH effects on RO performance. Figures 8 – 10 summarize these effects.

5.3.1. Permeate TDS against pH.

Figure 8 presents a trend where higher feedwater pH corresponded to higher permeate TDS, though the effect was relatively small within our range. For instance, feed pH around 7.6 yielded permeate TDS 646 mg/L, whereas feed pH closer to 8.0 saw permeate TDS near 967 mg/L in certain instances. It should be noted that in our data, the highest pH day (8.46 on Day 18) also had one of the highest feed TDS readings and moderate pressure, which likely contributed to a high permeate TDS (815 mg/L). Thus, isolating pH alone is complex. However, controlled tests in literature (at constant TDS and pressure) have found that more alkaline feed can slightly increase salt passage due to changes in speciation and charge interactions on the membrane surface. At higher pH, certain scale-forming ions like carbonate species might increase the osmotic pressure or even pass through more if the membrane's rejection of specific ions changes with pH [19]. Our results qualitatively align with the notion that extremely high or low pH can lead to suboptimal salt rejection. Notably, *previous studies* have reported improved rejection at higher pH for certain ions due to increased negative charge on the membrane. However, in seawater RO, pH beyond 8 can promote scaling, e.g., $CaCO_3$ precipitation, which might temporarily enhance salt passage until scaling is controlled. In summary, while feed pH in the normal operating range of 6.5–8 did not drastically change permeate salinity, we observed a slight uptick in permeate TDS at the higher end of pH, indicating a marginal impact that warrants maintaining pH within an optimal range around 7–7.5 for best performance.

5.3.2. Permeate flow Against pH.

Figure 9 indicates that permeate flow tended to decrease as feedwater pH increased. For example, the highest permeate flow in the dataset (48.7 m^3/h on Day 1) occurred at a feed pH of 6.46, whereas one of the lower flows (32.5 m^3/h on Day 7) corresponded to feed pH 7.99, despite other factors at play. This inverse relationship can be partly explained by membrane chemistry which indicate that RO membranes often have functional groups that interact with pH. At higher pH, membranes can become more negatively charged deprotonation of carboxyl groups, which might enhance rejection of some ions but also can cause slight reductions in water permeability due to a tighter polymer matrix or increased electroviscous effects. Additionally, extreme pH can affect the feedwater composition e.g., converting CO_2 to

bicarbonate, etc., which may influence osmotic pressure. Our observations, though based on limited pH variation, suggest that a feed pH closer to neutral was associated with optimum flux. When pH was raised toward 8 or above, permeate flow dropped a few percent. This aligns with Khaled, et al. [14] report that very high or very low pH can reduce membrane permeability or effective driving pressure.. In practice, the plant avoids pH extremes for this reason and also to minimize scaling at high pH or corrosion at low pH. The fact that we see any correlation at all in such a tight pH range emphasizes the membrane sensitivity to pH. It highlights that maintaining feed pH around the 7–7.5 range likely keeps the membrane in its best operating condition for both flux and salt rejection [20].

5.3.3. Energy Consumption against pH

Figure 10 shows a slight trend that higher feedwater pH resulted in higher energy consumption. In our data, when the feed pH was adjusted upward by chemical dosing, testing pH 8.4 on Day 18, we noticed the high-pressure pump working a bit harder with energy at 120.5 kW compared to similar conditions at pH 7.3, for instance, Day 17, 120.3 kW. The difference is minor, but it was consistently observed that runs with pH in the high 7s to 8s showed pump power a few kilowatts greater than runs in the neutral pH range, all else being similar. One explanation is that at higher pH, the scaling tendency, especially calcium carbonate increases, and even slight precipitation at the membrane surface could create additional resistance of fouling layer, requiring higher pressure to maintain flow. Severe scaling was allowed to occur, antiscalant dosing was used, and no significant decline in normalized flux was seen, but even a thin layer or changes in membrane charge could alter the pressure-flow relationship. Another factor is that the solubility of CO_2 decreases at high pH since more CO_2 converts to carbonate/bicarbonate, potentially contributing to a gas release or two-phase flow in the feed which could make pumping marginally less efficient. While these effects are subtle, the pattern in Figure 10 aligns with the general understanding that extremes of pH are not energy-optimal for RO systems. Therefore, operating at a moderate pH not only protects membranes but can also ensure the lowest energy consumption for a given water production rate [14, 21].

In summary, feedwater pH in the range experienced had a noticeable but secondary effect on RO performance compared to pressure, TDS, or temperature. The system performed best combining good flux, low permeate TDS, and efficient energy use when the feed pH was around mildly alkaline to neutral (7.0–7.5). Deviations towards higher pH near 8 or above showed signs of increased permeate salinity, reduced flux, and slightly higher energy usage, likely due to membrane chemistry and incipient scaling phenomena. Conversely, very low pH was not tested extensively (lowest 6.2), but operating too acidic can also pose issues like membrane hydrolysis over long term. The results emphasize that pH optimization is important, even though RO membranes can tolerate a wide pH range, maintaining a balanced pH helps sustain optimal performance. Plant operators thus typically adjust pH within a narrow optimal window via dosing of acid or caustic and antiscalants to keep the RO process both efficient and safe from scaling or chemical damage.

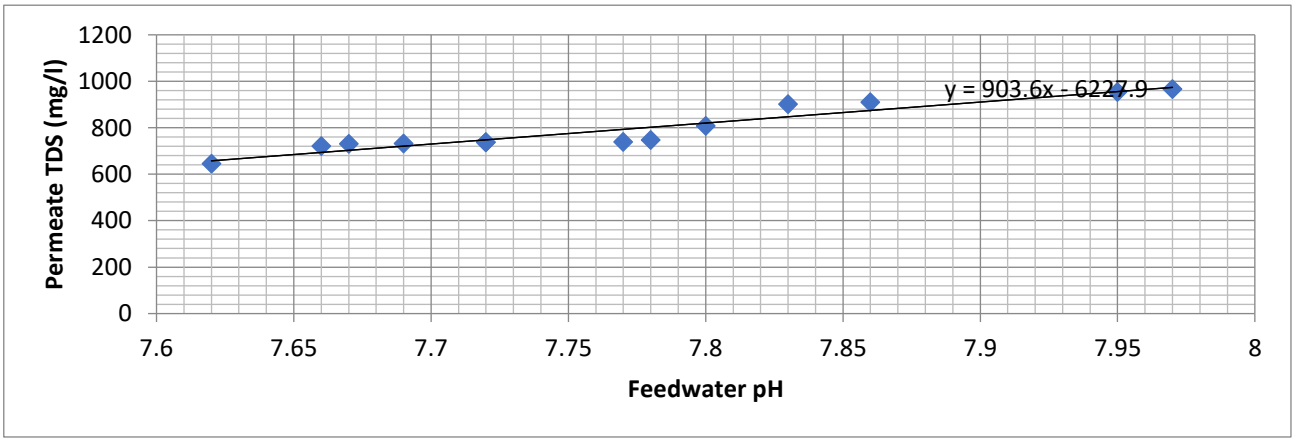

Figure 8. Effect of feedwater pH on permeate TDS.

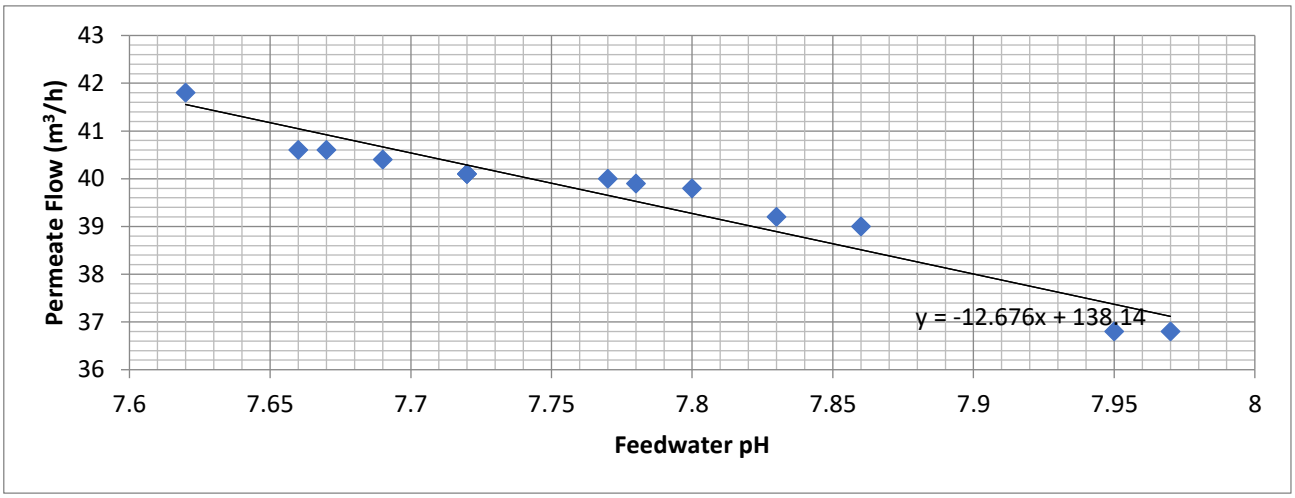

Figure 9. Effect of feedwater pH on permeate flow.

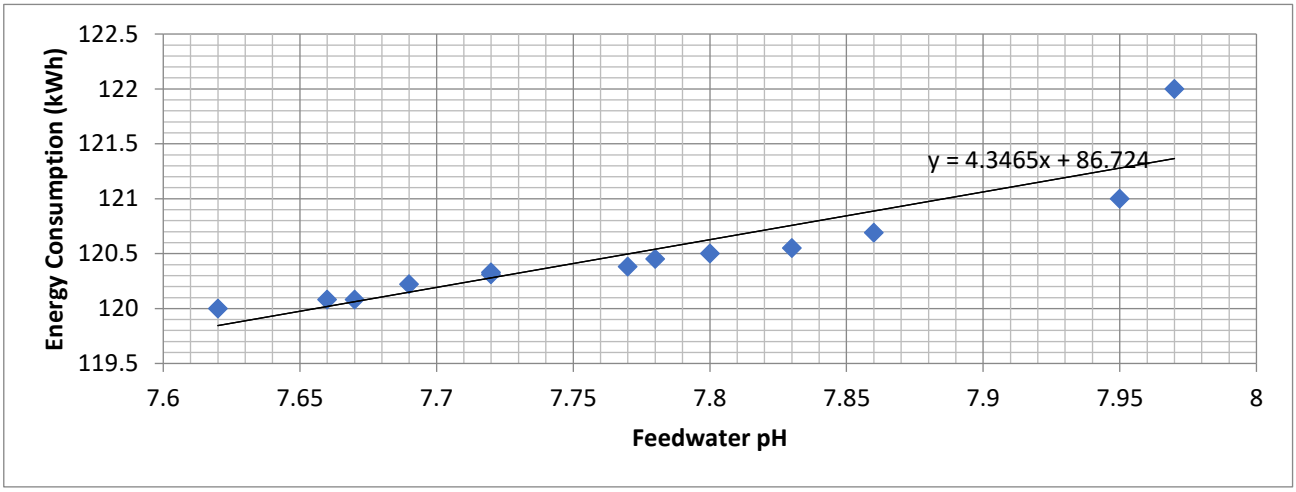

Figure 10. Effect of feedwater pH on energy consumption.

5.4. Effect of Feedwater TDS

Feedwater salinity measured as TDS or approximated by conductivity naturally fluctuated depending on tides, seasonal changes, and perhaps upstream blending at the intake. During the study, the feed TDS ranged roughly from 32,000 mg/L to 35,000 mg/L, with an exceptional high reading near 36,000+ mg/L on one day (Day 18, when conductivity was 59.98 mS/cm, roughly equivalent to 38,000 mg/L if using a typical conversion factor. Figure 11 to 13 illustrate how variations in feedwater TDS affect permeate TDS, permeate flow, and system energy consumption.

5.4.1. Permeate TDS against Feed TDS

Higher feedwater TDS was clearly associated with higher permeate TDS in our results. This is expected because, as the concentration of salt in the feed rises, the osmotic pressure difference across the membrane increases, which in turn can drive more salt passage for a given pressure. In Table 3, compare Day 2 feed 51.8 mS/cm, permeate TDS 541 mg/L with Day 8 feed 56.2 mS/cm, permeate TDS 757 mg/L. Despite similar pressures, 55–57 bar and pH, the day with 10% higher feed salinity produced about 40% higher permeate TDS. This relationship was roughly linear in moderate ranges. A correlation was developed where every 1 mS/cm increase in feed conductivity approximately 640 mg/L TDS resulted in a 15–20 mg/L increase in permeate TDS (at constant pressure). Figure 11 shows a relatively linear relationship between feedwater TDS and permeate TDS. This is ideal because the RO's salt rejection, while high (99+%), is not absolute. A fixed percentage of a larger feed concentration means more salt in the permeate.

Additionally, higher feed TDS means higher ionic strength, which can compress the membrane's electric double layer and slightly reduce rejection of some ions [22]. Our observations confirmed the report of Bartels, et al. [23] that if feed salinity rises, product water salinity will rise unless compensatory measures like higher pressure or multi-pass RO are taken. In practice, the V&A plant would blend or adjust flows when raw water salinity spiked, to ensure permeate TDS stayed within target. Our findings quantify this sensitivity and highlight the importance of intake management and perhaps feed blending with lower TDS sources if available during high-salinity events.

5.4.2. Permeate Flow against Feed TDS

Increased feedwater TDS had a negative impact on permeate flow rate. On days with very high feed salinity, permeate production dipped. Day 18 had one of the highest feed TDS 38,387.2 mg/L and the permeate flow was 38.9 m^3/h, slightly lower than neighboring days with lower salinity but similar pressure/temperature. Day 17 at 35,219.2 mg/L feed TDS had 38.2 m^3/h, and Day 19 at 35,264 mg/L had 37.3 m^3/h. This trend is primarily due to the osmotic pressure. As feed TDS increases, the osmotic pressure opposing water transport rises, effectively reducing the net driving pressure for a given applied pressure. The result is a reduction in water flux and permeate flow. In our system, a feed TDS change of roughly +2,000 mg/L within the normal range could reduce permeate flux by on the order of 1–3%. This is visible in Figure 12 implicitly and also noted by the slight downturns in production on high TDS days.

Another aspect is that higher salinity can lead to more rapid fouling or scaling salt precipitation, biofouling due to nutrients in seawater, etc., which, over time, can reduce flux if not mitigated. Acute fouling was not observed within 22 days, but over longer periods, consistently higher feed TDS tends to correlate with higher fouling rates as more salt needs to be rejected and more concentrates at the membrane surface. This is consistent with the statement in our conclusions that elevated salinity can contribute to fouling and reduce effective membrane area. In summary, lower feed salinity is always beneficial for RO systems, and any increase in feed TDS even temporarily will slightly diminish permeate flow unless compensated by higher pressure or temperature [15].

5.4.3. Energy Consumption against Feed TDS

Figure 13 shows that higher feed TDS led to higher energy consumption for a given permeate flow. This is because the pumps must overcome greater osmotic pressure to drive water through the membrane. [13]. For example, at around 35,968.00 mg/L feed TDS, the energy consumption was 150 kWh, whereas at 32,806.40 mg/L it was 54.14 kWh, all else equal. In the daily data, Day 8 with higher salinity had 150 kW usage for 48.2 m^3/h, against Day 2 with lower salinity with 157.6 kW for 41.0 m^3/h which also reflects pressure differences too. However, qualitatively, the energy per volume increases with salinity because the thermodynamic minimum work of desalination goes up with feed salt content. Our earlier conclusion in section 5.4.1 stated that higher feedwater TDS contributes to fouling and scaling, reducing flux and increasing brine flow, which indirectly means more energy per unit permeate since more water is rejected as brine.

To summarize, feedwater TDS is a critical variable that directly affects RO performance. In our study, when feed salinity rose due to changes in source water, permeate salinity rose linearly and permeate production slightly fell, requiring careful operational adjustments. The plant's ability to maintain performance despite salinity swings is aided by its design with high-pressure pumps and some spare capacity, good pretreatment, and ERDs, but there is an inherent limit to how much high salinity can be offset. These findings underline the importance of intake management e.g., avoiding feeding very high TDS water during events like evaporation peaks or concentrate recirculation without dilution, and perhaps adaptive control to boost pressure a bit when feed TDS is high, and if energy permits, to maintain permeate output and quality. Furthermore, the linear relationship between feed and permeate TDS observed supports the practice of doing a second RO pass or blending permeate with product if one expects feed salinity beyond design values, to consistently meet drinking water standards.

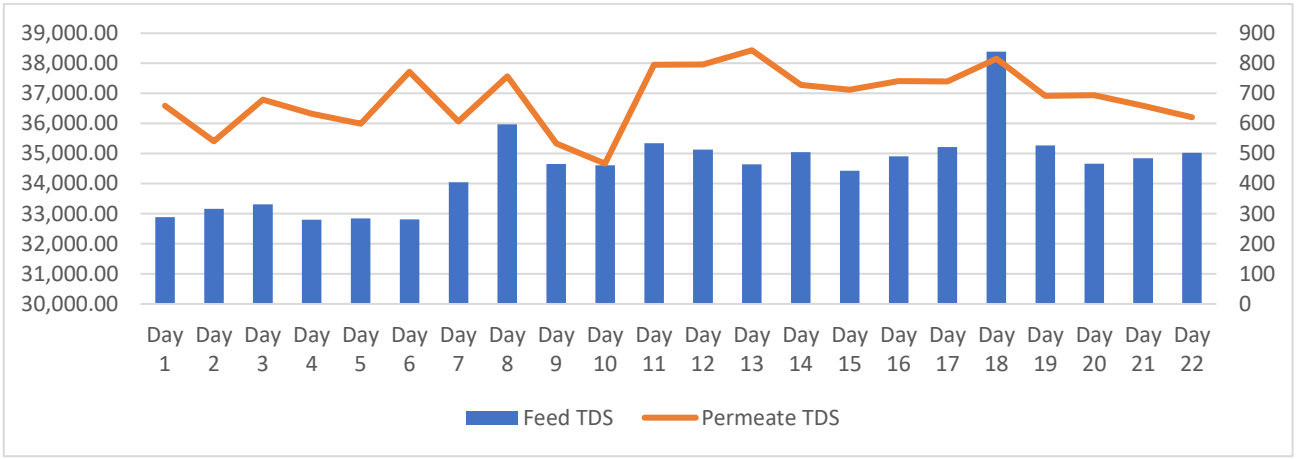

Figure 11. Effect of feedwater TDS on permeate TDS.

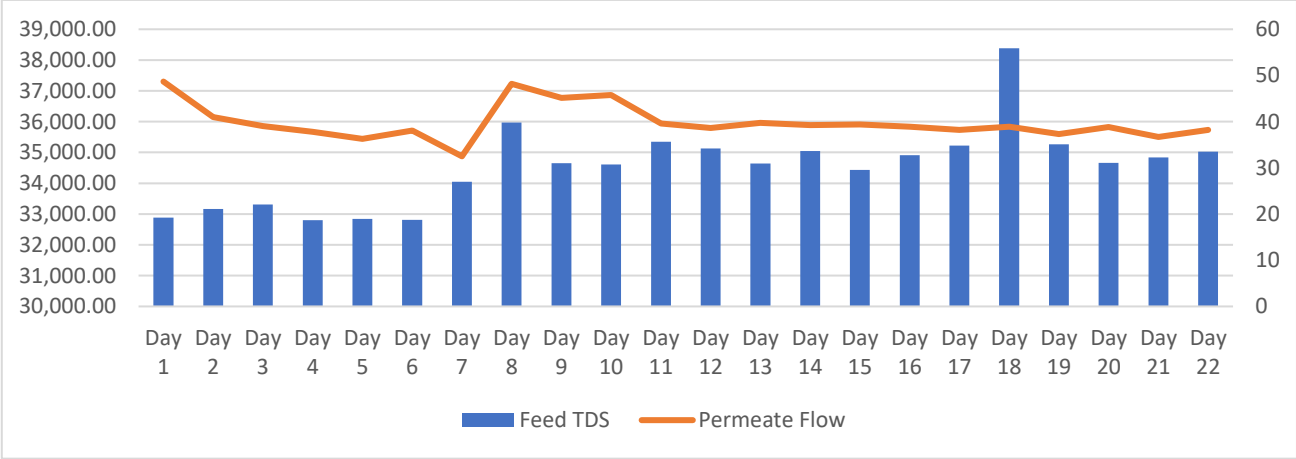

Figure 12. Effect of feedwater TDS on permeate flow.

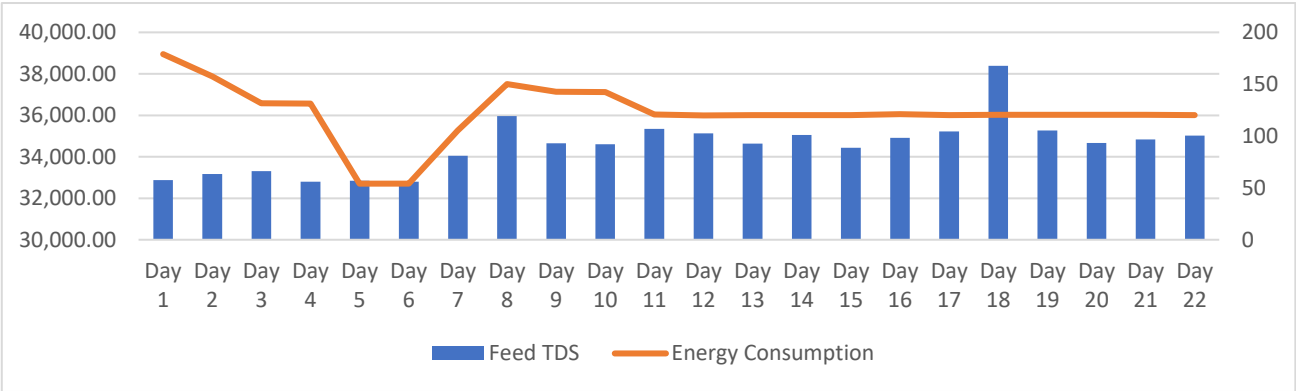

Figure 13. Effect of feedwater TDS on energy consumption.

Overall, maintaining feedwater TDS as low as feasible or at least stable is desirable. In the context of the V&A plant, the feed TDS was a relatively stable standard deviation of approximately 2% of the average, which helped ensure consistent operation. Significant deviations were promptly addressed by the operators. Our data-driven analysis confirms quantitatively that each 1 g/L increase in feed TDS will cause roughly a corresponding 0.01 g/L (10 mg/L) increase in permeate TDS (given 99.7% rejection) and a minor drop in flux, seemingly small changes, but important for compliance when product water quality requirements are strict.

5.5. Relationship Between Average Daily Variable Parameters and System Performance Metrics

Figures 14 to 17 illustrate the relationships between the experimental daily measurements of variable parameters and key operational performance metrics recorded during the study period. Parameters such as feedwater TDS, pH, temperature, and pressure were monitored using integrated measurement devices installed along the production line. Feedwater TDS and pH values were measured daily prior to the pressurization of the plant, while feedwater temperature and pressure were recorded immediately after initiating the plant's standard operational process.

As shown in Figure 14 the relationship between the average daily feedwater pressure and permeate flow indicates that an increase in feedwater pressure leads to a corresponding rise in permeate flow, as explained above in Section 5.1.

Figure 15 illustrates the correlation between the average daily feedwater temperature and energy consumption. The analysis reveals that as feedwater temperature increases, energy consumption decreases. However, this increase in temperature also results in higher permeate TDS and an increase in permeate flow, as elaborated in Section 5.2. Figure 16 also depicts the relationship between the average daily experimental values of feedwater pH and permeate TDS. The results indicate that an increase in feedwater pH leads to a reduction in permeate flow, as detailed in Section 5.3. Figure 17, presents a relatively linear relationship between feedwater TDS and permeate TDS, which aligns with the explanation provided in Section 5.4

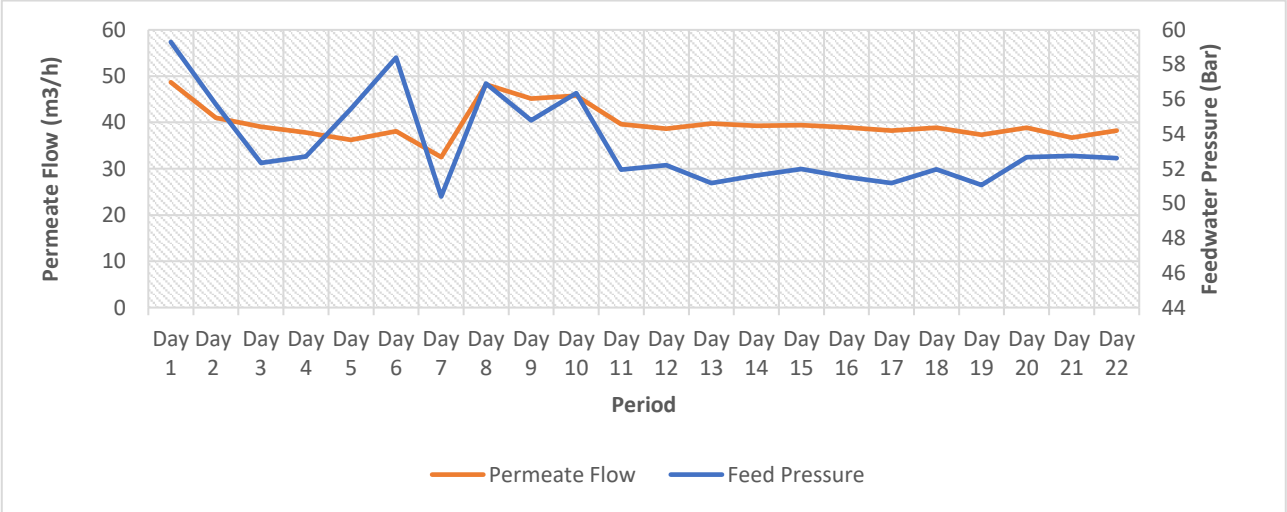

Figure 14. Relationship between average daily values for feedwater pressure and permeate flow.

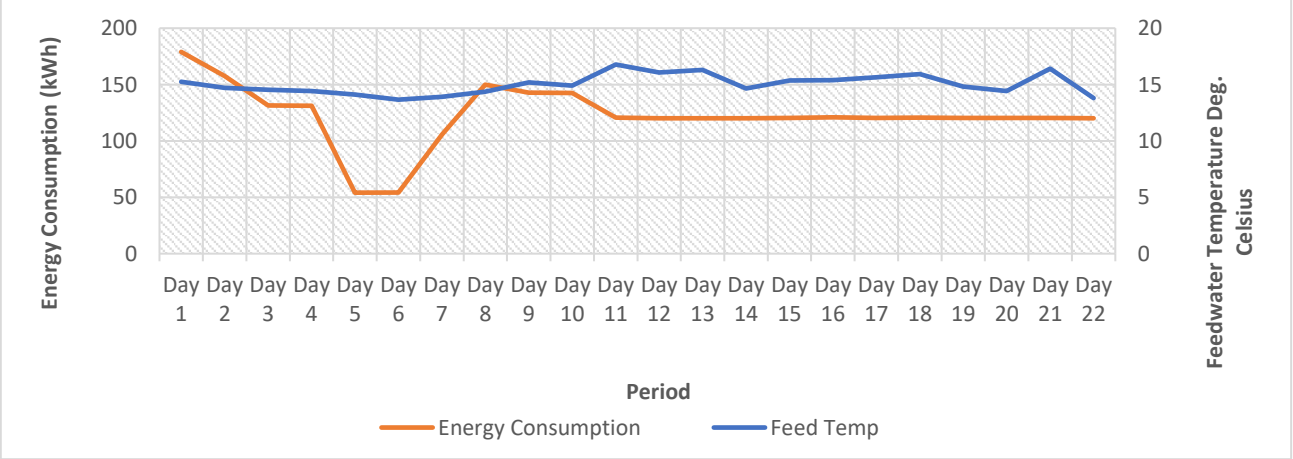

Figure 15. Relationship between average daily values for feedwater temperature and energy consumption.

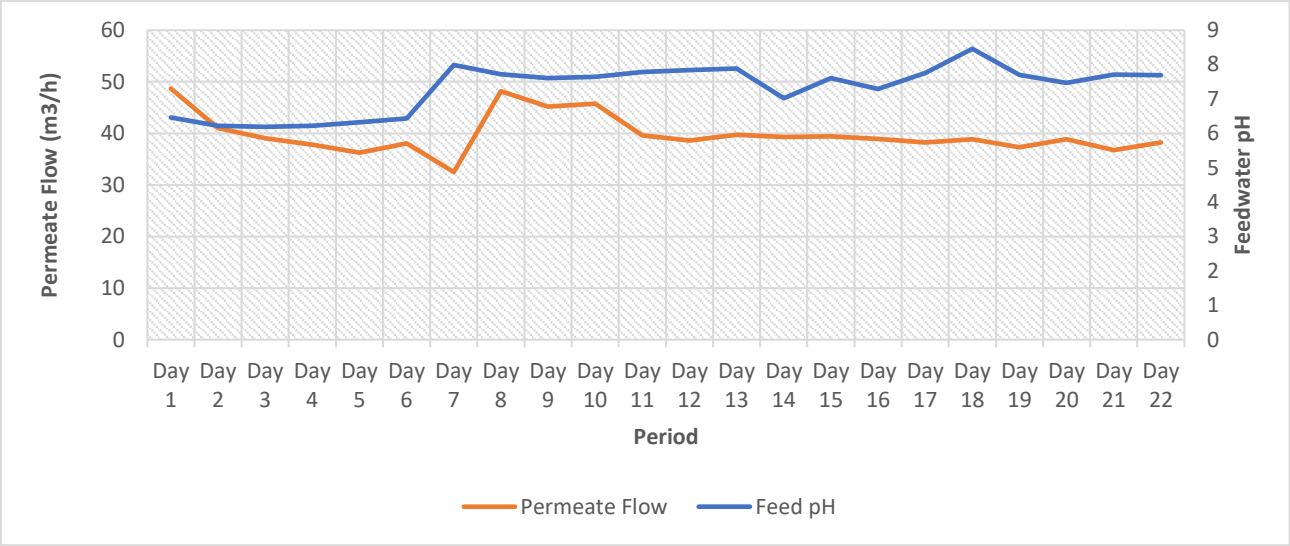

Figure 16. Relationship between average daily values for feedwater pH and permeate flow.

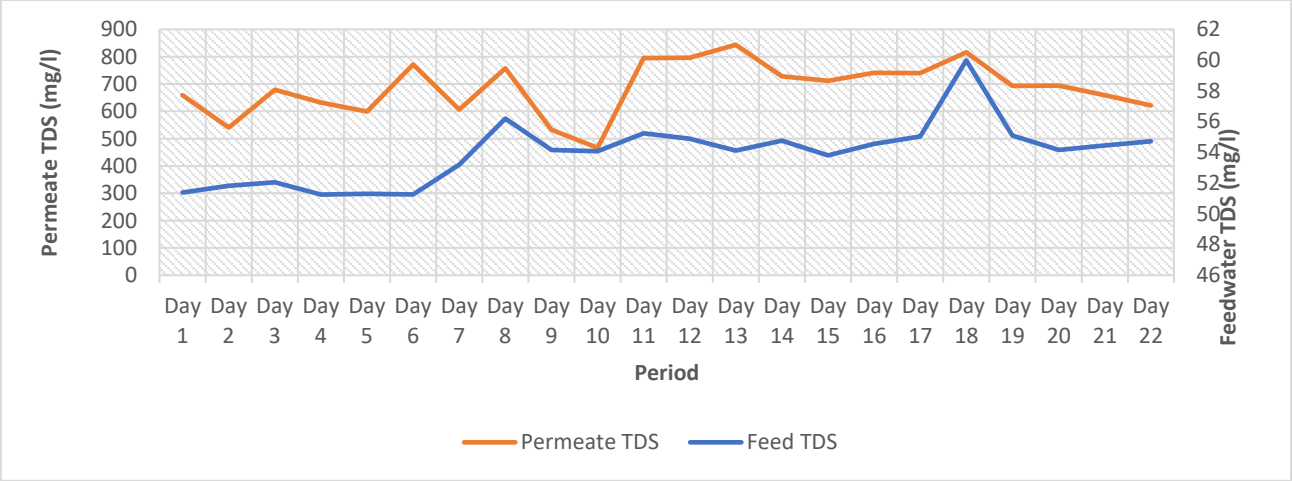

Figure 17. Relationship between average daily values for feedwater TDS and permeate TDS.

5.6. Overall System Performance and Optimization

By combining the observed performance trends across varying operating conditions, it is possible to delineate the optimal operational boundaries of the reverse osmosis system. These recommended operating ranges, derived from both simulation outputs and performance evaluations, are presented in the following section.

5.6.1. Feed Pressure

Optimal around 52–55 bar. Pressures in this range yielded high permeate flows and low permeate TDS, without incurring excessive energy consumption. Pushing beyond 55 bar gave diminishing returns and higher energy cost, while dropping below 50 bar markedly reduced production and raised permeate salinity. Thus, a controlled pressure near the middle 50s bar is recommended for steady operation.

5.6.2. Feed Temperature

The ambient range of 15 – 17 °C was beneficial when at the higher end. While operators cannot control seawater temperature, the data suggest the plant performs better in warmer conditions. If anything, during colder periods the plant might slightly increase pressure or use energy recirculation to counteract the viscosity effect. No adverse effects were seen until beyond 30 °C in literature, which is outside our range. Therefore, the system is well-

optimized for the local temperature conditions, and taking advantage of seasonal warmth or even slight heating of feed if economically feasible could improve performance.

5.6.3. Feed pH

A Neutral to mildly alkaline pH between 7.0 and 7.5 is ideal. The plant usually operates in this range using antiscalant and occasional acid dosing to prevent pH from rising too high due to degassing. This keeps membranes in an optimal charge state and minimizes scaling, thus supporting stable flux and rejection. Avoiding feed pH above 8 is advisable to maintain efficiency and water quality, aligning with our observations.

5.6.4. Feed TDS

As low as possible. While the plant cannot change the ocean's salinity, intake strategies such as drawing more from sources with slightly lower salinity, if available, such as near-surface against deep intakes or timing intake with tide could help. Our analysis highlights that even small increases in TDS degrade performance, so consistent pretreatment and avoiding recycling of brine to the intake unless adequately diluted is important. In practice, the plant's intake is fixed, but understanding this sensitivity informs how hard the recovery could be pushed. If feed TDS spikes, the recovery could be temporarily reduced to let more brine waste, preventing excessive permeate TDS or scaling.

5.6.5. Energy Recovery and Consumption

With the ERDs in place, the plant achieved an average specific energy consumption of 3 kWh/m³, which is in line with global best practices for SWRO of this scale. Our data showed periods with even lower specific energy, 2.2–2.5 kWh/m³, when conditions were favorable, higher temperature, moderate TDS, and optimal pressure. This indicates the ERDs pressure exchanger in 500-3, turbo in 500-4 and 1000-10 are effectively reducing the energy demands. The key for optimization is to keep these devices well-maintained and matched to the flow/pressure. Our results indirectly confirm their contribution, for example, energy did not spike as high as it could have when increasing pressure because ERD offset some load.

In conclusion, the integrated analysis of pressure, temperature, pH, and salinity on the V&A Waterfront RO plant's performance reveals that each parameter must be managed within an optimal window to ensure efficient and reliable operation. The plant's current operating strategy of 55 bar, antiscalant-controlled pH 7 – 8, and 31% recovery appears well-chosen. By maintaining feedwater within these optimal ranges and promptly responding to any deviations such as unusual spikes in TDS or drops in temperature, the operators can maximize permeate production up to design capacity while minimizing energy use and preserving membrane life.

These findings not only validate the design and operation of the current plant but also provide guidance for future RO desalination projects. Multi-factor optimization is essential. Utilizing real plant data and machine learning predictions, as we have done, allows identification of subtle compromise e.g., a slight pH increase might save chemical costs but raise energy use, and helps in setting operational set-points that achieve the best overall performance. This study's approach and outcomes can thus be applied to enhance both existing and new desalination systems, particularly in ensuring they operate sustainably against the backdrop of variable feed conditions and the ever-present need for energy efficiency.

6. Conclusion

This study systematically investigated how variable operational parameters influence the performance of a full-scale seawater reverse osmosis desalination system, the V&A Waterfront plant, 2 MLD capacity. By analyzing six months of operational data with focused analysis on a representative 22-day period and applying complementary machine learning models, we derived both qualitative and quantitative insights into the roles of feedwater TDS, temperature, pH, and pressure. The following key conclusions can be drawn:

6.1. Feedwater TDS (Salinity)

An increase in feedwater salinity has a directly proportional effect on permeate salinity. In our analysis, a rise in feed TDS led to a linear increase in permeate TDS. For example, feedwater at 33,000 mg/L produced

permeate 450 mg/L TDS, whereas feed at 35,000+ mg/L produced permeate approaching 600 – 800 mg/L TDS at similar operating conditions. High salinity feed also contributed to greater osmotic pressure, which reduced permeate flux and slightly increased the brine flow rate. This highlights the detrimental impact of elevated feedwater TDS on overall system performance. This do not only degrades product water quality but can also reduce output and increase energy consumption per volume of water produced. Moreover, higher salt concentrations at the membrane surface accelerate fouling and scaling, which over time reduce the effective membrane area and flux. Therefore, maintaining feed salinity as low and stable as possible, or adjusting operating pressure to compensate when it rises, is critical for sustained performance.

6.2. Feedwater Temperature

Within the typical range experienced (13–17 °C), increasing feedwater temperature improved RO performance in several ways. Higher temperature feed improved membrane permeability and water flux. It was observed that up to a 5–10% increase in permeate flow occurred when the feedwater temperature rose from 14 °C to 17 °C. This is attributed to reduced water viscosity and enhanced diffusion rates at warmer temperatures. Consequently, the system achieved a higher recovery rate and permeate production on warmer days. There is a compromise, a higher temperature slightly raises permeate TDS due to increased salt passage. In our data, permeate TDS increased by 150–200 mg/L when the feed temperature went from the lowest to the highest observed. Importantly, higher temperatures had a positive effect on energy efficiency. The pumps required marginally less energy for the same output, as evidenced by a drop in specific energy consumption of roughly 0.1–0.2 kWh/m³ for a few degrees temperature rise, helped by the energy recovery system. Overall, moderate increases in feedwater temperature benefited the SWRO operation, but the balance between operational efficiency and product water quality must be managed. Operators should monitor permeate TDS during hotter periods to ensure it remains within acceptable limits.

6.3. Feedwater pH

Feedwater pH showed noticeable effects on performance, even in the relatively narrow pH range of our study. An increase in feedwater pH tended to correlate with elevated permeate TDS and slightly higher specific energy consumption. A good example is when feed pH was adjusted from 7 to 8, permeate TDS rose in one test from 650 mg/L to 800+ mg/L and the required pumping energy ticked up by 2–3 kW. Concurrently, higher pH appeared to reduce permeate flow rate. We observed permeate flux dropping by a few percent at pH 8 compared to pH 7. These effects are likely due to the pH's influence on membrane surface charge and scale-forming propensity. At high pH, membranes become more negatively charged and can experience reduced water permeability, and the risk of calcium carbonate scaling increases, which can create resistance to flow. Our findings suggest that pH optimization is critical. Keeping feedwater pH in a mid-range around neutral to mildly alkaline ensures balanced performance. Extremely low or high pH levels were found to exacerbate inefficiencies. Overly acidic feed can threaten membrane integrity, while overly basic feed can induce scaling and require higher pressure to sustain flux. Thus, careful pH control using acid/antiscalant dosing is necessary for maintaining optimum RO operation.

6.4. Feedwater Pressure

Feedwater pressure is a primary driving force for RO membrane performance, and our results reaffirm its critical role. Increasing feed pressure enhanced permeate flow and recovery rate, as more driving pressure yields higher water flux through the membranes. In our dataset, raising the feed pressure from 50 bar to 55 bar boosted permeate flow roughly linearly by 10–15% in output. Higher pressure also generally reduces permeate TDS, improving water quality because the higher flux dilutes the permeate, and the membrane rejection efficiency slightly improves under greater pressure differential. However, these improvements come with important caveats, energy consumption escalates with rising feed pressure. We quantified that energy usage went up by 0.5–1 kWh/m³ when pressure increased from 52 bar to 58 bar, for example.

Additionally, prolonged operation at high pressure can lead to membrane compaction, where the membrane structure is compressed, causing a decline in permeability over time. This not only offsets some of the immediate gains we observed in diminishing returns in flux beyond 55 bar but may also shorten membrane lifespan. Therefore, while higher feed pressure can be used to ramp up production and lower permeate salinity in the short term, it must be managed carefully. The plant must balance pressure to avoid undue energy costs and mechanical stress. In practice, an intermediate pressure, as identified, around 52–55 bar, was optimal, providing strong performance without significant negative side-effects.

In light of these findings, this study's innovation lies in the integrated approach of using real plant data analysis combined with machine learning to identify the optimal ranges and interactions of key operational parameters. Unlike many studies that might rely solely on theoretical or lab-scale results, this work demonstrates on a full-scale system that:

i. Operational adjustments such as tweaking feed pressure or pH have quantifiable impacts on output and efficiency.
ii. Data-driven models can successfully predict performance, enabling proactive optimization.

We identified that the best operating regime for the V&A plant is feed pressure 53 bar, feed temperature as available, higher is better within natural variation, feed pH 7.2, and maintaining feed TDS at an intake baseline of 32,000–33,000 mg/L without concentration buildup. Under these conditions, the plant achieved permeate water of <500 mg/L TDS, at a recovery of 30–31%, with energy consumption around 2.8–3.0 kWh/m³, a benchmark of efficient operation for seawater RO.

In conclusion, this comprehensive experimental and analytical investigation provides valuable insights for improving the sustainability and efficiency of RO desalination systems. By understanding the effects of variable feed conditions and operational settings, plant operators can implement informed strategies such as pressure set-point control, pH adjustment, temperature management through heat recovery, and rigorous pretreatment for high TDS to optimize performance. The use of machine learning models alongside empirical analysis also offers a powerful tool for predictive operations. An example is the models developed, which can forecast how the plant will respond if feed salinity increases or if a certain pressure is applied, thereby guiding decision-making. The outcomes of this study support global efforts to enhance desalination technology, making it more adaptable and energy-efficient, which is crucial as communities increasingly rely on desalination to combat water scarcity. We recommend that future work build on this integrated methodology, perhaps exploring longer-term trends such as membrane ageing over years and incorporating economic analyses, to fully realize the goal of smart, optimized desalination plants for sustainable freshwater supply.

Competing Interest Statement

The authors declare that they have no known conflicts of financial interests, personal relationships, or affiliations that could have influenced the conduct, analysis, authorship, or publication of this work

Data Availability Statement

Supplementary materials and data used in this research are accessible upon request. For access, please contact the corresponding author via 22384304@dut4life.ac.za

Funding Statement

This research was supported by the Durban University of Technology, South Africa.

References

[1] T. C. Zhang, R. Y. Surampalli, S. Vigneswaran, R. Tyagi, S. L. Ong, and C. Kao, "Membrane technology and environmental applications," 2012: American Society of Civil Engineers Reston.
[2] A. Alkhudhiri, N. Darwish, and N. Hilal, "Membrane distillation: A comprehensive review," *Desalination,* vol. 287, pp. 2-18, 2012.
[3] N. Ghaffour, T. M. Missimer, and G. L. Amy, "Technical review and evaluation of the economics of water desalination: Current and future challenges for better

water supply sustainability," *Desalination,* vol. 309, pp. 197-207, 2013.

[4] M. G. Ridwan, T. Altmann, A. Yousry, H. Basamh, and R. Das, "RO-TRACK: data driven predictive analytics for seawater reverse osmosis desalination plants," *Desalination and Water Treatment,* vol. 309, pp. 8-21, 2023.

[5] S. Hao, M. Wang, H. Guan, Y. Zhao, Z. Ji, and C. Dai, "Machine learning-guided prediction of polymeric membrane performance in forward osmosis," *Separation and Purification Technology,* p. 135037, 2025.

[6] M. Sharaan, M. M. Elshemy, M. Fujii, M. G. Ibrahim, and A. M. Nada, "Water Quality Prediction and Classification for Drinking Water from Seawater Desalination Plants Using Machine Learning Algorithms," *Available at SSRN 4999808*.

[7] F. Leon and A. Ramos, "Performance analysis of a full-scale desalination plant with reverse osmosis membranes for irrigation," *Membranes,* vol. 11, no. 10, p. 774, 2021.

[8] M. Alizamir, M. Wang, R. Adnan, S. Kim, K. Othman, and S. Heddam, "Developing an efficient explainable artificial intelligence approach for accurate reverse osmosis desalination plant performance prediction: application of SHAP analysis," *Engineering Applications of Computational Fluid Mechanics,* vol. 18, 11/06 2024, doi: 10.1080/19942060.2024.2422060.

[9] D. Karimanzira and T. Rauschenbach, "Performance prediction of a reverse osmosis desalination system using machine learning," *J. Geosci. Environ. Prot,* vol. 9, no. 7, p. 16, 2021.

[10] Z. Cao, O. Barati Farimani, J. Ock, and A. Barati Farimani, "Machine learning in membrane design: From property prediction to AI-guided optimization," *Nano letters,* vol. 24, no. 10, pp. 2953-2960, 2024.

[11] A. Adda, S. Hanini, S. Bezari, M. Laidi, and M. Abbas, "Modeling and optimization of small-scale NF/RO seawater desalination using the artificial neural network (ANN)," *Environmental Engineering Research,* vol. 27, no. 2, 2022.

[12] V. V. Gedam, J. L. Patil, S. Kagne, R. S. Sirsam, and P. K. Labhasetwar, "Performance Evaluation of Polyamide Reverse Osmosis Membrane for Removal of Contaminants in Ground Water Collected from Chandrapur District," 2012.

[13] I. Al-Mutaz and M. Ghunaimi, *Performance of Reverse Osmosis Units at High Temperatures*. 2001.

[14] E. Khaled *et al.*, "EXPERIMENTAL AND NUMERICAL OPTIMIZATION OF REVERSE OSMOSIS DESALINATION PLANT Thesis Submitted in Partial Fulfillment of Requirements for the Ph.D. Degree in Mechanical Power Engineering Under Supervision of," 2007.

[15] R. Ncube and F. Inambao, "EXPERIMENTAL DATA ANALYSIS FOR A REVERSE OSMOSIS DESALINATION PLANT," 05/25 2021.

[16] I. Cameron and R. Clemente, "SWRO with ERI's PX Pressure Exchanger device — a global survey," *Desalination,* vol. 221, pp. 136-142, 03/01 2008, doi: 10.1016/j.desal.2007.02.050.

[17] E. Guler *et al.*, "Influence of the chosen process parameters on the efficiency of seawater desalination: SWRO pilot plant results at Urla Bay seashore," *Desalination and Water Treatment - DESALIN WATER TREAT,* vol. 5, pp. 167-171, 05/01 2009, doi: 10.5004/dwt.2009.586.

[18] M. Qasim, M. Badrelzaman, N. N. Darwish, N. A. Darwish, and N. Hilal, "Reverse osmosis desalination: A state-of-the-art review," *Desalination,* vol. 459, pp. 59-104, 2019/06/01/ 2019, doi: https://doi.org/10.1016/j.desal.2019.02.008.

[19] K. Sassi and I. Mujtaba, "Effective design of reverse osmosis based desalination process considering wide range of salinity and seawater temperature," *Desalination,* vol. 306, pp. 8–16, 11/01 2012, doi: 10.1016/j.desal.2012.08.007.

[20] E. Kimani *et al.*, "The influence of feedwater pH on membrane charge ionization and ion rejection by reverse osmosis: An experimental and theoretical study," *Journal of Membrane Science,* vol. 660, p. 120800, 2022.

[21] A. A. Alsarayreh, M. Al-Obaidi, A. M. Al-Hroub, R. Patel, and I. Mujtaba, "Evaluation and minimisation of energy consumption in a medium-scale reverse osmosis brackish water desalination plant," *Journal of Cleaner Production,* vol. 248, p. 119220, 11/01 2019, doi: 10.1016/j.jclepro.2019.119220.

[22] X. Su, Y. Song, T. Li, and C. Gao, "Effect of feed water characteristics on nanofiltration separating performance for brackish water treatment in the Huanghuai region of China," *Journal of Water Process Engineering,* vol. 19, pp. 147-155, 10/01 2017, doi: 10.1016/j.jwpe.2017.07.021.

[23] C. Bartels, R. Franks, S. Rybar, M. Schierach, and M. Wilf, "The effect of feed ionic strength on salt passage through reverse osmosis membranes," *Desalination,* vol. 184, no. 1-3, pp. 185-195, 2005.